Glass Transition Thermodynamics and Kinetics

Frank H. Stillinger[1] and Pablo G. Debenedetti[2]

[1]Department of Chemistry, [2]Department of Chemical and Biological Engineering, Princeton University, Princeton, New Jersey 08544; email: fhs@princeton.edu, pdebene@princeton.edu

Annu. Rev. Condens. Matter Phys. 2013. 4:263–85

First published online as a Review in Advance on January 3, 2013

The *Annual Review of Condensed Matter Physics* is online at conmatphys.annualreviews.org

This article's doi:
10.1146/annurev-conmatphys-030212-184329

Keywords

Kauzmann temperature, ideal glass transition, potential energy landscape, dynamical heterogeneity, inherent structures

Abstract

The remarkable kinetic slowdown experienced by liquids as they are cooled toward their glass transition is not accompanied by any obvious structural change. Understanding the origin of this behavior is a major scientific challenge. At present, this area of condensed matter theory is characterized by an abundance of divergent viewpoints that attempt to describe well-defined physical phenomena. We review representative theoretical views on the unusual kinetics of liquid supercooling, which fall into two broad competing categories: thermodynamic and kinetic. In the former, an apparent "ideal," thermodynamic, glass transition caused by rapid loss of entropy in the supercooled liquid underlies kinetic slowdown; in the latter, purely kinetic constraints are responsible for loss of ergodicity. The possible existence of an ideal thermodynamic glass transition is discussed and placed in its proper statistical mechanical context.

1. INTRODUCTION

The enormous diversity of condensed matter systems that we experience in daily life typically includes materials that have not attained a state of complete thermal equilibrium. Many of these materials exhibit properties that change very slowly with the passage of time; some even appear to be time independent, and so can be empirically classified as permanently occupying metastable states. Specifically, these metastable substances include both natural and manufactured glassy (vitreous) solids that have been generated from liquids cooled rapidly through, and well below, their respective thermodynamic melting points, thus bypassing crystal nucleation. Quantitative understanding of what the time-dependent formation processes create for the resulting atomic or molecular-scale structure, and macroscopic observable properties, of the low-temperature metastable state constitutes important scientific, technological, and industrial objectives. Many basic questions in this area remain unanswered. In particular, the fundamental issue of whether observed liquid-to-glass transitions are only a slowed-kinetics phenomenon or are actually a thermal precursor of an obscured "ideal" phase transition remains a vigorously debated topic.

The glass-forming properties to be considered here are relevant to chemically very diverse substances. They range from elements to high-molecular-weight polymers and include important examples of both inorganic and organic materials as pure substances and as mixtures. Some colloidal suspensions qualify for inclusion because experimentally they also can exhibit glass transitions. However, certain classes of amorphous materials are excluded from the review. These exclusions cover amorphous solids produced by vapor-phase deposition, disrupting a crystal phase with severe mechanical deformation, or intense radiation damage; materials generated by such processes have not normally been considered in theoretical studies of glass transition phenomena.

It is a testament to the creativity of the research community that an impressive variety of nominally distinct visions for glass phenomena have been advanced. On account of length constraints, the objective here is to examine very briefly a representative sample of the competing views. These bear specifically on the unusual kinetics encountered during liquid supercooling and on the possible existence of "ideal" glass transitions.

Precisely defined models for many-body phenomena obviously play a vital role in condensed-matter science. This is especially true in the glass transition context. Nevertheless, it is important to keep in mind a relevant but sobering fact: It is simply that the power of mathematics permits the construction of many-body models whose exact (approximation-free) properties can extend well beyond realistic physical behavior. This situation needs specifically to be appreciated with respect to the ideal glass transition debate. A related concern is that the mathematical character of approximations applied to analysis of physically reasonable models can analogously generate vivid but physically unrealistic predictions.

The published scientific literature devoted to experimental observations of glass formers and their interpretations is enormous. This compact review of glass transition theoretical viewpoints is constrained to be very selective in its focus, so it necessarily skips over many details. Consequently, interested readers may find it useful to consult some of the previously published review articles for additional relevant information concerning both experimental observations and theoretical approaches for glassy materials (1–9).

Section 2 provides some basic historical background for the glass transition subject. Section 3 presents a few basic statistical mechanical concepts useful for a comprehensive description of the out-of-equilibrium states inhabited by glassy materials. Section 4 surveys some recent views of kinetic slowdown processes that lead to observable glass transitions. Section 5 examines the

viewpoint according to which ideal glass transitions might exist in principle. Section 6 covers some relevant aspects of energy landscape topography. Section 7, Conclusions, brings this review to a close.

2. HISTORICAL BACKGROUND

As precise experimental calorimetry became available in the past century, it was then feasible and inevitable for a wide variety of supercooled liquids and the glasses they form to be examined in detail and with increasing accuracy. In particular, this permitted reproducible measurements of isobaric (constant pressure) heat capacities $C_p(T)$ for many supercooled liquids down to their empirical glass transition regions ($T \approx T_g$), at which their internal relaxation times begin suddenly to exceed practical measurement times, typically occurring in the $10^2 - 10^3$s range. A widely cited review article by Kauzmann (10) identified basic questions concerning the relation between those attainable supercooled states and the thermodynamically stable crystal phases whose nucleation and growth out of the liquid were bypassed by sufficiently rapid cooling. In particular, Kauzmann stressed that the distinctly higher heat capacity normally exhibited by the liquid compared to its crystal, which persists and usually magnifies upon supercooling down to the experimental glass transition temperature T_g, raises basic questions about the relative entropy of the two macroscopic states in the low-temperature limit.

Figure 1 schematically illustrates the situation addressed by Kauzmann. **Figure 1*a*** presents the isobaric molar heat capacities of the crystal ($C_{p,c}$) and of the liquid ($C_{p,l}$) branches (including both the stable and the metastable supercooled portions) as functions of the absolute temperature. This figure includes an elementary extrapolation of the liquid portion below T_g. **Figure 1*b*** presents the correspondingly implied entropy difference $\Delta S(T) = S_l(T) - S_c(T)$ for T at and below the equilibrium melting temperature T_m. This result is based on the measured equilibrium heat of melting, and the entropy change upon further cooling at the prevailing pressure, which is represented by a temperature integration involving the C_p curves:

$$\Delta S(T) = \Delta S(T_m) - \int_T^{T_m} [C_{p,l}(T') - C_{p,c}(T')](dT'/T'). \qquad 1.$$

The primary inference from this simple procedure is that the entropy difference between the crystal phase and the supercooled liquid (if indeed it could be reproducibly equilibrated below T_g) apparently would vanish linearly as a function of $T - T_K$ at a Kauzmann temperature $0 < T_K < T_g$. An analogous temperature integration indicates that the enthalpy of the extrapolated liquid would remain significantly above that of the crystal at T_K, implying that structurally the two phases would remain distinct, a conclusion also supported by density extrapolation. Kauzmann stressed the paradoxical implication of further extrapolation below T_K toward $T = 0$, which would require that a configurationally disordered liquid medium possess a lower entropy than its periodically ordered crystal phase. This state of affairs would lead to a liquid with negative absolute entropy at $T = 0$. This paradox, and eventual violation of the third law of thermodynamics, would be eliminated if the disordered glass exhibited an "ideal" higher-than-first-order phase transition at T_K, below which it would remain substantially structurally unchanged, as does the crystal.

The situation illustrated in **Figure 1** implicitly assumes that only a single thermodynamically stable crystal phase for a substance of interest is present over the entire temperature range $0 \leq T \leq T_m$. There are of course cases in which two or more crystal-crystal phase transitions occur

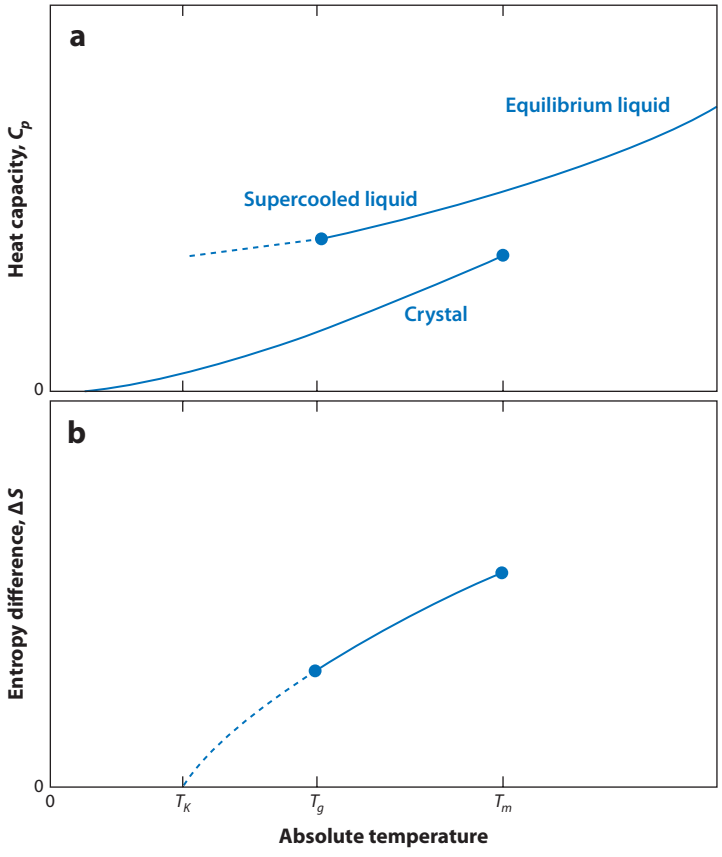

Figure 1

Qualitative view of supercooled liquid versus stable crystal thermal properties. (*a*) Measurable and extrapolated values of isobaric heat capacities for the equilibrium liquid ($T \geq T_m$), supercooled liquid ($T < T_m$), and the equilibrium crystal ($0 \leq T \leq T_m$). The dashed line indicates a simple extrapolation below the experimental glass transition temperature T_g. (*b*) Implied entropy difference between the phases, including the sub-T_g extrapolation to a Kauzmann temperature T_K at which the entropy difference apparently vanishes.

in equilibrium at the relevant pressure. Well-known examples include order-disorder transitions, such as those presented by ammonium chloride and its deuterated variant (11). In such circumstances, the required extension of Equation 1 involves the heat of transition for a first-order polymorphic crystal phase change, or a proper accounting of a possible heat capacity divergence at a higher-order phase change. One also needs to keep in mind that crystal phases can occasionally retain frozen-in structural disorder, thus departing from thermodynamic equilibrium, a textbook example of which is the hydrogen-bond disorder in hexagonal ice, with residual entropy approximated long ago by Pauling (12).

Kauzmann's suggestion for removal of the paradox involved the temperature dependence of crystal nucleation rate within the temperature-extended supercooled liquid (10). He indicated that the free energy barrier for the nucleation would approach zero at a temperature above T_K, thus producing an uncontrollably high rate for that nucleation. Consequently, he concluded that the supercooled liquid could not maintain its individuality down to T_K, and so no physical significance should be attached to the alternative possibility of an ideal glass phase transition occurring near

T_K. However, more recent experimental studies of homogeneous crystal nucleation have shown that its rate as a function of supercooling temperature decrement tends first to pass through a maximum and then to plunge rapidly toward zero as $T \to 0$ (13). Consequently, sufficiently rapid cooling through this temperature interval of maximum nucleation rate can in principle lead to survival of an unnucleated supercooled liquid medium, thus circumventing the Kauzmann suggestion. This seemingly restores the possibility of an entropy-vanishing scenario and its implication for the existence of an ideal glass transition at or close to T_K to avoid the Kauzmann entropy paradox. The heat capacity of an ideal glass below its transition temperature would contain only vibrational contributions, similar to the crystal phase situation in the same temperature range.

The tentative identification of a thermodynamically meaningful Kauzmann temperature as illustrated in **Figure 1** is nominally based on static measurable thermal properties of glass-forming substances. The possibility that such a singular point defined by vanishing of the static property ΔS might have broader implications received support from the temperature behavior of measurable kinetic properties for the supercooled liquids involved. These kinetic properties include shear viscosity η, mean shear-stress and thermal relaxation times $\overline{\tau}_{shear}$ and $\overline{\tau}_{thermal}$, and the self-diffusion constant D. In the supercooled liquid, the temperature variations of these properties tend to deviate from simple Arrhenius form, often exhibiting remarkably rapid variation as temperature declines toward the T_g range. As a result, measurements of these properties historically have been fitted at least approximately to the generic Vogel-Tammann-Fulcher (VTF) functional form:

$$\eta(T), \overline{\tau}_{shear}(T), \overline{\tau}_{thermal}(T), D^{-1}(T) \approx A \exp\left[\frac{C}{T - T_0}\right]. \qquad 2.$$

Here A has at most a weak temperature dependence, and C and T_0 are positive constants. These three parameters for a given substance can vary according to the temperature range of fitting considered. The extent to which measurements adhere to, or deviate from, pure Arrhenius ($T_0 = 0$) behavior has provided the basis for classifying glass formers on a "strong" versus "fragile" scale (4, 13, 14); one possible measure of this "strength" property for the data range of interest is simply the dimensionless quantity C/T_0. The formal divergence of the empirical VTF expression at T_0 for glass formers has often been observed to lie very close to their Kauzmann temperature T_K, suggesting therefore that this might not be random coincidence, but additional circumstantial evidence for the existence of an ideal glass transition at positive temperature (Reference 15, figure 4). In other words, the basic $\Delta S = 0$ static criterion for an ideal glass transition may indeed be automatically accompanied by singularities in kinetic properties. Nevertheless, it should be noted in passing that analysis of more recent experimental studies has questioned whether a VTF-type divergence is supportable (16).

The nominally distinct Kauzmann static thermodynamic analysis and the VTF-type representation for kinetic properties were in effect bridged by the appearance of the Adam-Gibbs relation (17). Its underlying concept is that relaxation and flow processes in the deeply supercooled liquid regime proceed via local structural excitations that occur within essentially independent cooperatively rearranging regions (CRRs) inside the supercooled medium. This can be viewed as a precursor of the dynamical heterogeneity concept (18). The number of CRRs was presumed to be roughly proportional to the inverse of their average volume over the temperature range $0 < T < T_m$. Furthermore, the mean value of that size for these CRRs, as well as of their excitation free energies, was argued to be inversely proportional to $\Delta S_{conf}(T)$, the difference in entropy between the liquid and crystal phases that is attributable to nonvibrational degrees of freedom. Thus, it was concluded that the average value of a typical relaxation time would have the following form:

$$\overline{\tau} \approx \overline{A} \exp\left[\frac{\overline{C}}{T\Delta S_{conf}(T)}\right]. \quad 3.$$

It has also been argued that the vibrational contributions to the entropies of the two phases tend to be close enough so their difference can be neglected (17), and thus it would be reasonably accurate to replace $\Delta S_{conf}(T)$ by $\Delta S(T)$ in this Adam-Gibbs relation. Consequently, if the inference that the latter entropy difference vanishes at a $T_K > 0$ is correct, then indeed this would be coupled to divergence of measurable relaxation rates, and of the macroscopic shear viscosity η. That the configurational entropy difference might vanish linearly at a positive temperature was supported by an approximate enumeration of linear polymer configurations by Gibbs & DiMarzio (19).

It has long been recognized empirically that the structural relaxation rates for supercooled liquids representing time-dependent responses to various mechanical, thermal, and electrical perturbations can deviate significantly from simple exponential relaxation. In particular a frequently invoked representation of time-dependent response involves a stretched-exponential function, also known as the Kohlrausch-Williams-Watts (KWW) relaxation function (20, 21):

$$f_\theta(t) = \exp\left[-(t/\tau)^\theta\right]. \quad 4.$$

Here θ is a fractional exponent lying in the range $0 < \theta \leq 1$, and τ sets the overall timescale of the relaxation being described. As temperature in a liquid declines from well above T_m, into the supercooled regime, and toward its experimental T_g, fits to response data have typically shown $\theta(T)$ to decline from approximately unity to values approaching 1/2, while the corresponding $\tau(T)$ rises strongly (4). The reasons why the stretched-exponential form arises have historically been a subject of debate. However it is worth noting that this form mathematically can result from a superposition of simple exponential contributions with different decay rates; this formally can be revealed by expressing $f_\theta(t)$ as a Laplace transform:

$$f_\theta(t) = \int_0^\infty F_\theta(s) \exp(-st) ds. \quad 5.$$

Here $F_\theta(s) > 0$, and this function can be expressed in closed form for at least some θ values (22). Nevertheless, the existence of this Laplace transform resolution does not prove that the basic kinetic processes producing the system's net relaxation response are merely simple exponential relaxations.

The vanishing of the entropy difference $\Delta S(T)$ between liquid and crystal phases occasionally occurs within the thermodynamic equilibrium regime. Such occurrences are intrinsic to the inverse melting phenomenon, for which the slope of the continuous and differentiable equilibrium melting curve $p_m(T)$ in the temperature-pressure plane changes sign (23). In this circumstance, adding heat isobarically to the liquid at coexistence causes crystallization. The helium isotopes provide examples at low temperature, and at much higher temperature poly(4-methylpentene-1) also exhibits inverse melting (24). Although unrelated to the glass formation phenomenology, the occurrence of equilibrium states with vanishing entropy difference between crystal and liquid phases implies that this phenomenon by itself carries no implications for dynamics. A detailed analysis of the vibrational contributions to crystal and liquid entropies for the above-mentioned substances would be needed to verify unequivocally for them the corresponding logical decoupling between ΔS_{conf} and relaxation kinetics.

3. STATISTICAL MECHANICAL CONTEXT

The remarkable growth of computing power over the past few decades has provided valuable support to analytical theory of glass transition phenomena. This has led to the introduction and numerical simulation of a broad range of many-body models. Proper interpretation of model properties relating to glass transitions, whether generated analytically or via powerful numerical simulation, requires adherence to the basic principles of statistical mechanics. A few key aspects of those principles that are directly applicable to liquid metastability and glass transition phenomena are now presented. To keep the discussion relatively simple, electronic conductors (i.e., metallic glasses) are excluded.

It is obvious that quantum mechanics is fundamentally involved in determining atomic and molecular structures for glass-forming substances and in determining interparticle potential energies operating within those substances. But beyond that, quantum phenomena do not play an essential role in determining the kinetic or structural aspects of glass formation. However this does not exclude the important role of quantum mechanics in cryogenic properties of glasses, such as two-level-system tunneling contributions to heat capacity (25, 26), in determining thermal conductivity, as well as establishing intensities measured by spectroscopic probes for glassy media [such as those revealing boson peaks (27)]. Nevertheless, for the present review classical statistical mechanics will suffice to describe supercooling and glass formation. In principle, it can also serve to evaluate the various theoretical approaches now available and to determine what additional insights would be required to "complete" the subject.

Within this classical context, the observable state of a many-particle system at time t can be described in terms of a normalized probability distribution function $f(\mathbf{R}, \mathbf{P}, t)$:

$$\int d\mathbf{R} \int d\mathbf{P} f(\mathbf{R}, \mathbf{P}, t) = 1, \qquad 6.$$

where $\mathbf{R}$ stands for the full collection of configurational coordinates (e.g., positions of all atom nuclei), and $\mathbf{P}$ is the set of conjugate momenta. Specifically, f represents the phase-space distribution for an ensemble of systems with identical compositions and nominally identical histories prior to observation time t. To describe thermodynamically metastable states such as supercooled liquids, those histories may need to include removal of those individual ensemble members that prior to time t have exhibited undesirable nucleation of the thermodynamically more stable phase.

Time evolution of $f(\mathbf{R}, \mathbf{P}, t)$ reflects the system's dynamics that is under the control of the interactions present. These include both intramolecular and intermolecular interactions, as well as occasional coupling to a heat bath to impose a cooling (or heating) schedule. It is assumed that the electronic-insulator substances under consideration have a bounded (but possibly large) molecular weight. For these glass formers, the intrasystem interactions can be represented by a many-particle potential energy function $\Phi(\mathbf{R})$. The isochoric (constant volume V) thermal equilibrium situation at temperature T involves a canonical distribution function f whose configurational part contains the Boltzmann factor $\exp[-\Phi(\mathbf{R})/k_B T]$, where k_B is Boltzmann's constant. For isobaric conditions (constant pressure p) that often apply to experimental investigations, the corresponding configurational Boltzmann factor in f is $\exp[-\Psi(\mathbf{R}, V)/k_B T]$, where

$$\Psi(\mathbf{R}, V) = \Phi(\mathbf{R}) + pV. \qquad 7.$$

The behavior of any many-particle system, whether under a cooling schedule or otherwise, is profoundly influenced by the multidimensional topography of the Φ hypersurface (isochoric

conditions), or alternatively the Ψ hypersurface (isobaric conditions), on which the system dynamically evolves. This topography varies drastically depending on the chemical nature of the system. It typically includes a complicated distribution of local and global minima (inherent structures), as well as saddle points of varying orders (i.e., classified by their numbers of negative curvatures). These extrema fall into equivalence classes defined by permutations of identical particles and by the particles' intramolecular symmetries, if any.

When interest focuses on the liquid-phase supercooling regime, the portion of configuration space that describes substantial crystallinity is by convention excluded from consideration. A theoretical device to enforce this protocol involves erecting an impenetrable barrier within the multidimensional configuration space that separates the amorphous liquid-like configuration subset from the nucleated and crystal-grown subset. Consequently, the glass-forming systems of interest inhabit, and are confined to, only the former subset. **Figure 2** presents a simplified cartoon-like representation of such a barrier inclusion in the configuration space.

The interactions within most atomic and molecular systems (accounting for electrostatic shielding of ions) are short ranged in real space. This underlies a basic conclusion that the number of distinct types of Φ and Ψ minima (inherent structures) in their respective multidimensional spaces rises exponentially with N, the number of particles present, even when those minima are classified by depth on a per-particle basis (28). Because the elementary transitions between neighboring basins surrounding minima involve just local particle rearrangements in an extended system (29, 30), only $O(N)$ such transitions can be expected to occur in a typical observation period. Consequently no single macroscopic system under observation will dynamically explore any but a miniscule fraction of the available basins within the full Φ or Ψ topography. Thus, the notion of a single system being at "equilibrium" only implies that its classical dynamics has visited a tiny but accurately representative sample of the available basin set that is relevant at the prevailing observational conditions. By contrast, individual liquid systems supercooled below their respective glass transition temperatures will also sample only miniscule fractions of the available basins; however, in that case the sampling is far from representative for the prevailing temperature.

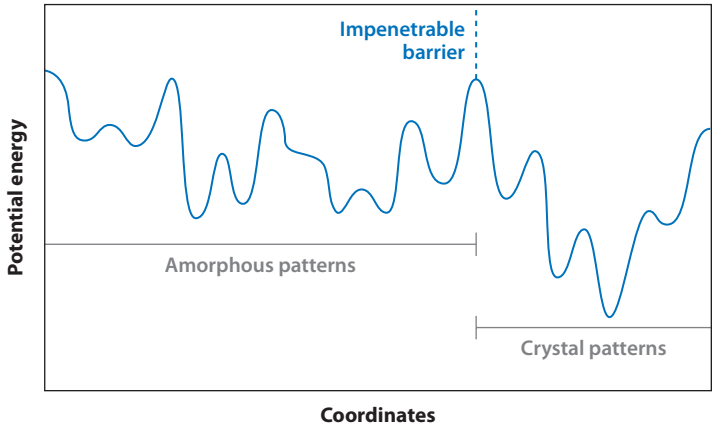

Figure 2

Simple graphical representation of an impenetrable barrier erected in multidimensional configuration space to prevent nucleation and crystal growth in supercooled liquid samples. Although nominally representing isochoric (constant volume) circumstances, a similar situation applies to isobaric (constant pressure) circumstances where the coordinate set includes volume as a variable and potential energy is replaced by potential enthalpy (**Equation 7**).

Whether isochoric or isobaric conditions prevail, the time-dependent entropy for a classical ensemble described by $f(\mathbf{R},\mathbf{P},t)$ can be assigned using the following functional:

$$S(t)/k_B = C(N) - \int d\mathbf{R} \int d\mathbf{P} f(\mathbf{R},\mathbf{P},t) \ln f(\mathbf{R},\mathbf{P},t). \quad 8.$$

The leading term $C(N)$ comprises absolute-entropy contributions that are independent of interactions and arise from the classical limit of the underlying quantum statistical mechanics; it cancels in expressions for entropy differences between phases. In the single-component structureless-particle case residing in $d = 3$ dimensions, this term becomes

$$C(N) = -\ln(h^{3N}N!), \quad 9.$$

where h is Planck's constant. Equation 8 reduces to the conventional entropy definition for classical ensembles under thermodynamic equilibrium conditions. Individual members of an ensemble that has been cooled toward absolute zero will end up localized permanently in a single Φ or Ψ basin surrounding an inherent structure, but that is not what the entropy measures; it is instead a measure of the breadth of distribution across inequivalent inhabited basins for the entire ensemble of systems.

4. KINETIC SLOWDOWN DESCRIPTIONS

A general question that must be confronted is what configurational rearrangements in three dimensions are feasible in a supercooled liquid, given the extremely complicated $\Phi(\mathbf{R})$ or $\Psi(\mathbf{R}, V)$ multidimensional topographies for the full set of many-body interactions that are present. In particular, as the temperature declines, why do those molecular motions exhibit such vivid rate slowing compared to the timescale of experimental observation? It might be esthetically pleasing to have a straightforward universal answer covering all glass formers (31). However, in examining analytical and numerical-simulation modeling it is important to keep open the possibility that the relevant description may depend qualitatively on what subfamily of glass formers is under consideration, given the wide diversity of molecular structures and their interactions.

Theoretical interpretations of the dramatic slowdown of structural relaxation in supercooled liquids fall into two broad categories, depending on how they are initiated conceptually. One focuses on time-dependent phenomena exclusively, and ascribes no causal or underlying role to thermodynamics. In sharp contrast, the thermodynamic viewpoint sees kinetic slowdown as a consequence of an underlying ideal glass transition.

The mode-coupling theory (MCT) offers a natural starting point for discussion of kinetic slowdown mechanisms in glass-forming substances (32–36). This approach is based on the Mori-Zwanzig formalism (37, 38) to describe the time dependence of density fluctuations at the atomic or molecular level. Upon invoking a two-mode closure approximation for the memory kernel involved, the MCT generates an explicit prediction for the intermediate scattering function in a liquid, which for wavevector length $k = |\mathbf{k}|$ is defined as follows:

$$F(k,t) = N^{-1}\langle \rho(\mathbf{k},0)\rho(-\mathbf{k},t)\rangle,$$

$$\rho(\mathbf{k},t) = \sum_{j=1}^{N} \exp(i\mathbf{k}\cdot\mathbf{r}_j). \quad 10.$$

Here, the three-dimensional locations of the N particles forming the liquid are denoted by $\mathbf{r}_1 \ldots \mathbf{r}_N$. The closure approximation utilized requires only the temperature and density-dependent static structure factor $S(k) \equiv F(k, 0)$ for the liquid as basic input.

Under the closure approximation, the MCT description of the $F(k, t)$ decay as time increases is indicated qualitatively in **Figure 3**. At high temperature in the thermodynamically stable liquid, the decay at very short times represents short-displacement inertial motion, whereas at larger times it is close to a simple exponential decay as expected for untrapped Brownian-type motion. But as temperature declines into the supercooled liquid regime, a two-stage behavior emerges, the short-time portion of which represents limited displacements of particles permitted locally by surrounding neighbor-particle arrangements. However the later-time stage shown, appearing as a flat plateau of finite duration in the logarithmic-time plot of **Figure 3**, represents mean imprisonment time for particles that results from caging by immediate neighbors. For moderate supercooling, this plateau is terminated by eventual particle escape into surroundings. In contrast, at and below a singular temperature $T_c > 0$ (not to be confused with the typographically similar critical temperature for fluids), the predicted plateau extends to infinite time without decaying to zero. This MCT result implies that the system dynamics has become nonergodic for $T < T_c$: Particles are no longer able to diffuse freely but remain localized near their initial positions.

The plateau lifetime illustrated in **Figure 3** for $T > T_c$ is substantially the average structural relaxation time for the supercooled liquid. When experimentally determined relaxation times in the moderately supercooled regime are fitted to the MCT prediction, which is an algebraically divergent function with the form $(T - T_c)^{-\gamma}$ (8, 9), the result of that fitting implies $T_c > T_g$. Clearly this is contradictory and indicates that MCT fails to correctly incorporate the dominant physical mechanism(s) for structural relaxation in deeply supercooled glass formers. In spite of this obvious shortcoming, MCT appears to provide a reasonably acceptable description well above T_g, including the appearance of two-stage relaxation behavior of the intermediate scattering function

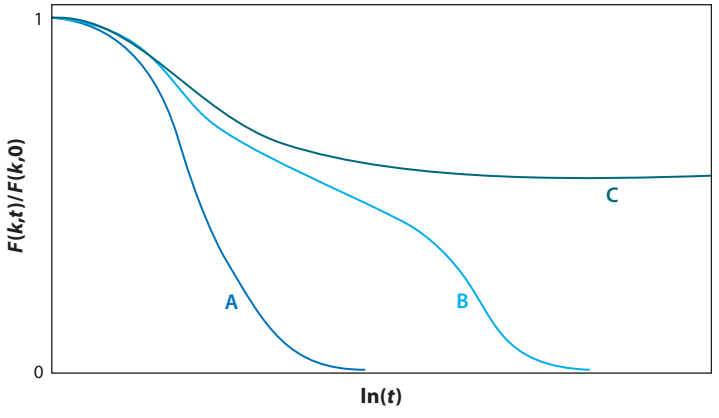

Figure 3

Schematic indication of development of the two-stage decay of the self-intermediate correlation function $F(k, t)$ plotted versus logarithm of elapsed time predicted by the mode-coupling theory (MCT). The wavevector magnitude k is intended to be close to its value producing the maximum of the structure factor $S(k) \equiv F(k, 0)$. Curve A represents the behavior in the hot liquid above its melting temperature; curve B illustrates appearance of a shoulder in a moderately supercooled liquid due to delayed escape from an instantaneous cage of neighbors; curve C illustrates the MCT prediction of nonergodicity at a $T_c > 0$, which extends the shoulder to infinite time.

$F(k,t)$, usually identified in conventional glass science as separation between β (short-time) and α (long-time) relaxation processes (5).

Wolynes and coworkers' random first-order transition theory (RFOT), or mosaic picture, is a thermodynamics-based theory of supercooled liquids and the glass transition (15, 39–41). Concepts incorporated in the original RFOT view of supercooled liquids are at least partly outgrowths of mean-field results for spin systems with interactions among the spins that have unlimited range and that incorporate quenched random disorder; these include the Sherrington-Kirkpatrick model (42), the Potts model (43), and the p-spin model (44). The RFOT pictures the glass as a collection of aperiodic mosaic structures. Under isochoric conditions, the free energy of a generic mosaic structure can be approximated using the following functional (Reference 15, equation 3):

$$\frac{F^{inh}[\rho(\mathbf{r})]}{k_B T} = \int d\mathbf{r}\rho(\mathbf{r})[\ln \rho(\mathbf{r}) - 1] + \frac{1}{2}\iint d\mathbf{r}d\mathbf{r}'[\rho(\mathbf{r}) - \rho_0][\rho(\mathbf{r}') - \rho_0]\varphi(\mathbf{r},\mathbf{r}'), \qquad 11.$$

where F^{inh} is a measure of the excess Helmholtz free energy due to density inhomogeneity compared to the spatially uniform state with density ρ_0, $\rho(\mathbf{r})$ is the nonuniform density, and $\varphi(\mathbf{r},\mathbf{r}')$ is a (dimensionless) interaction energy. The first term on the right-hand side captures the free energy cost associated with particle localization, and the second term is the corresponding energy contribution. Because particles execute mostly harmonic vibrations about their equilibrium positions in the long-lived aperiodic structure, one can postulate a density profile involving Gaussian displacements and a variational parameter α that quantifies the extent of localization. Upon substituting that variational profile into Equation 11, one finds that the free energy develops a metastable minimum with respect to α at sufficiently low temperatures or sufficiently high densities ρ_0. This corresponds to a first-order freezing transition. However, the actual transition advocated involves freezing into a very large set of aperiodic structures. The predicted result is a random first-order transition involving no enthalpy or volume discontinuity. As described (15), the aperiodic structures considered each appear to qualify as inherent structures on the Φ or Ψ landscape, but whether all or only a subset of those amorphous inherent structures are involved has not been precisely specified.

Connection with dynamics is subsequently established by considering the rate at which long-lived aperiodic structures can relax into liquid-like equilibrium configurations. The driving force for such a relaxation, namely, the multiplicity of liquid-like structures into which a local aperiodic solid can transform, is entropic. A penalty arises from the energy mismatch between the relaxing entropic droplet and the surrounding rigid mosaic of aperiodic crystals. Although a rigorous argument has yet to be provided, this mismatch energy has been stated to vary as the square root of the size of the entropic droplet (Reference 15, section 3.2). A number of predictions result about the dynamics and thermodynamics of glass-forming materials, including the relation between fragility and heat capacity discontinuity at the experimental glass transition; the temperature dependence of the characteristic cooperatively relaxing region's size, including the size of the cooperatively relaxing region at the glass transition; and the relation between fragility and stretched-exponential relaxation dynamics. Overall, the agreement with experiments is good (45, 46). Crucially, and with the exception of allegedly very small corrections (40), the RFOT approach infers divergence of relaxation times and a vanishing of configurational entropy at a common positive temperature $T_0 \equiv T_K$ (45, 47).

The increasing power and diversity of computer simulations for model glass formers in principle allow examination of growing length scales as temperature declines. Such statistical measures can be independent of, but qualitatively consistent with, the RFOT domain viewpoint.

One such proposed measure involves the point-to-set construction (47, 48). This procedure identifies a $\xi(T)$ as the minimum length scale at which a frozen bounding wall of particles fails to influence the interior of a surrounded particle-set configuration. Although a wide range of fixed particle configurations is available in principle, the most relevant choices in the present context amount to a frozen wall surrounding a convex, reasonably compact region. The results from applying this point-to-set technique indeed numerically establish a growing such length scale upon cooling but are not able to directly imply a divergence at some $T \geq 0$. In this context, a geometric frustration viewpoint has been developed, claiming that the domains in a mosaic structure have an intrinsic limitation to their size in simultaneously attempting to satisfy both low internal interaction energy as well as geometrically amorphous character (49), and if correct this eliminates singular behavior of all properties at a positive temperature T_K.

Computer simulations have been able to probe the $T \geq T_m$ equilibrium and $T < T_m$ moderately supercooled liquid states for a wide range of classical many-particle systems. Although currently available computing power is impressive, it is nevertheless restricted to examining short timescales and modest numbers of particles compared to those characterizing experiments on real substances. In spite of such limitations, some of these computer investigations have been successfully directed toward isolating and characterizing the elementary configurational transitions that produce relaxation and mediate flow processes. In particular, string-like collective motions have been identified in molecular dynamics simulations for some simple model glass formers. These motions involve a local group of particles whose neighbors displace in the same direction along the contour of an irregular path with an identifiable beginning and end. Binary Lennard-Jones models are the early source of such observations (50–52). Another study of this kind (53) has involved a single-component system whose particles interact via a Dzugutov pair potential (54); this is an interaction that predisposes particles to adopt local icosahedral coordination geometry, thus at least partially frustrating formation of spatially periodic crystalline order. The results obtained indicate that the average length of the string-like rearrangements increases as temperature is reduced.

Langer (55–57) has constructed a theory of glass transition phenomena that attributes a primary role to those string-like collective excitations, yielding a prediction of super-Arrhenius temperature behavior for relaxation and flow-process rates. This analysis views the string excitations as relocating amorphous-packing analogs of vacancies and interstitials, thus providing structural transitions between alternative packing configurations. To connect this concept to measurable kinetic phenomena, the approach derives free energies for string transitions as a function of their length and temperature, invoking a relevant interpretation of self-avoiding walks for the cooperative motions of the strings. This viewpoint has been presented as analogous to droplet growth in supersaturated vapors. It involves an increase in mean string length with decreasing temperature, and as a result predicts a corresponding reduction in rate of reconfiguration for the amorphous medium. The derived mean length diverges at a VTF temperature $T_0 > 0$, and the approach also identifies this as a positive temperature for vanishing of configurational entropy. Langer speculates that the string-like excitations may tend to be concentrated at grain boundaries between well-packed amorphous domains (57), with domain size diverging as temperature declines toward T_0.

A rather different viewpoint regarding kinetic slowdown has been proposed by Chandler and coworkers, advancing the notion of thermodynamics of trajectory space (58–60). Its development is based at least in part on the Fredrickson-Andersen facilitated kinetic Ising model (61), the Kob-Andersen kinetically constrained lattice model (62), and the Jäckle-Eisinger east model (63). This approach presents a locally coarse-grained description, including directional correlations between successive displacement events, of feasible particle displacements consistent with nonoverlap

constraints (64). The overall viewpoint stresses the importance of kinetics and does not invoke a thermodynamic phase transition of the conventional kind; i.e., it does not identify a Kauzmann temperature at which configurational entropy or a liquid versus crystal entropy difference suddenly vanishes. The resulting analysis does not quantitatively predict the drop in measured heat capacity as the relaxation timescale of a supercooled liquid exceeds available measurement times (65). However, the formalism generates a parabolic (in $1/T$) form for the logarithm of shear viscosities and mean relaxation times that offers superior fits to experimental measurements compared to VTF and other frequently used functional forms (66). This view of supercooled liquids identifies a nonequilibrium phase transition between ergodic and nonergodic phases in the space of trajectories (i.e., space and time) that produces kinetic retardation as temperature declines, thus providing an explanation for observable glass transitions. The configurational trajectories involve a kind of local geometric catalysis operating in regions of local particle mobility that become rarer as temperature declines. Although they are present and active in the low-temperature medium, the postulated mobility regions at any instant are viewed as embedded in a kinetically inert solid surrounding medium, described as space-time bubbles. That is, the basic many-particle pattern falls into the category of dynamic heterogeneity (18).

An impressive body of experimental results (67, 68) and a significant number of computer simulations (69–71) have been published supporting the dynamic heterogeneity concept for deeply supercooled glass formers. Specifically, they have demonstrated that elementary configurational rearrangements (such as the string-like displacements mentioned above) in a variety of model systems do not appear at random locations independently of what had just previously occurred. Instead, they tend to be clustered collectively into mobility domains that on average become fewer in number but grow in spatial extent and lifetime as temperature is lowered. Dynamic heterogeneity has been cited as underlying the failure of the Stokes-Einstein relation (72–74) which, if obeyed, would require the temperature variations of the self-diffusion constant D and the shear viscosity η for a single-component glass former to be such that $D\eta/T$ is temperature independent.

The spatial isolation of regions exhibiting anomalous mobility and their persistence over time are the intrinsic characteristics of dynamic heterogeneity. Consequently, it is natural to identify and quantitatively apply functions that are sensitive to this property. Families of four-point space-time correlation functions are well suited for this purpose, and are available to monitor dynamic heterogeneity as temperature and/or density vary in supercooled liquids (9, 18, 75). The four points of basic interest are the initial and final positions over time interval t for two particles whose centers are initially separated by distance r. As an example, let $f_j(t,0)$ be a measure of how far particle j moves between time 0 and time $t > 0$. Then the following is a time-dependent mobility field for an N-particle medium:

$$f(\mathbf{r},t,0) = \sum_{j=1}^{N} f_j(t,0)\delta\big[\mathbf{r} - \mathbf{r}_j(0)\big]. \qquad 12.$$

The relevant four-point correlation function then represents the dependence of mobilities of initially close-by pairs in the isotropic medium:

$$G_4(r,t) = \langle f(\mathbf{r},t,0)f(0,t,0)\rangle - \langle f(\mathbf{r},t,0)\rangle^2. \qquad 13.$$

The spatial integral of this function defines a dynamic susceptibility:

$$\chi_4(t) = \int d\mathbf{r} G_4(\mathbf{r},t). \qquad 14.$$

These measures of dynamic heterogeneity have been evaluated for several model glass formers, including the Kob-Andersen 80:20 Lennard-Jones binary mixture model (51), a different Lennard-Jones binary mixture at 50:50 composition (76), a polymer melt (77), and molten silica (78). When plotted versus ln t these $\chi_4(t)$ results exhibit a maximum that grows in height and is located at increasing time as temperature is lowered. This is just the behavior expected for dynamic heterogeneity involving domains of anomalous mobility that grow in average geometric size and lifetime as the extent of supercooling increases.

Additional information about collective motions in the dynamic heterogeneity scenario is available from the isoconfigurational ensemble approach (79, 80). This technique examines statistics of the set of trajectories that can develop in time from a given initial configuration, due to variation in initial Maxwell-Boltzmann velocity assignments. An important insight obtained via this analysis is the emergence of a spatially heterogeneous distribution of propensities for particle motion upon supercooling and the observation that the propensity distribution is encoded in the particle configuration, albeit in an as-yet not fully understood way. A numerical simulation applying the isoconfigurational ensemble approach to the Kob-Andersen binary Lennard-Jones model concludes that mobile particles exhibiting the highest average directionality tend to be located at interfaces between high and low mobility clusters (81).

Evidently strong repulsions operating between particles at small separations play an important role in the appearance of dynamic heterogeneity at low temperature. This is emphasized by examining the contrasting behavior of models incorporating soft-core pair potentials. The elementary Gaussian core model (GCM) at high density provides a clear example. Careful numerical study by molecular dynamics simulation (82) establishes that crystal nucleation becomes very improbable in the high-density regime for this model, thus allowing deep supercooling and a glass transition. But unlike many glass formers, the supercooled GCM fluid adheres well to the Stokes-Einstein relation (82), thus avoiding the deviations from that relation, which conventionally are interpreted as a signature of dynamic heterogeneity.

5. IDEAL GLASS TRANSITION ISSUES

The ideal glass transition historically has been identified with Kauzmann's vanishing of the entropy difference $\Delta S(T) = S_l(T) - S_c(T)$ described earlier in Equation 1. To be precise, the Kauzmann criterion for an ideal glass transition is the vanishing at a positive temperature T_K of $\Delta S(T)/N$ in the large system limit. Subsequent theory has employed variants of this criterion as convenient for identifying ideal glass transitions. Most frequently encountered is positive-temperature vanishing of the configurational entropy difference per particle in the infinite system limit, as mentioned earlier in connection with the Adam-Gibbs relation (Equation 3). This is justified by the fact that measured heat capacities of glasses below T_g, and of the corresponding crystal phases, each containing only vibrational contributions, tend to be quantitatively very close (e.g., see Reference 83 for *o*-terphenyl and Reference 84 for selenium). Consequently, very little shift in a predicted ideal glass transition would be involved. In principle, the equilibrium crystal has a small positive configurational entropy at any $T > 0$ due to extremely small concentrations of point defects (vacancies, interstitials), so that disregarding this feature and thus assuming $N^{-1}\Delta S_{conf} = N^{-1}S_{conf}(liq) = 0$ would be an adequate criterion for existence of an ideal glass transition at a positive temperature. These criterion distinctions are relatively minor issues, generally, for the subject of ideal glass transitions.

In view of the linkage that has often been made from experimental measurements between a possible Kauzmann temperature T_K inferred from static (thermodynamic) properties, and a rate-vanishing temperature T_0 suggested by kinetic behaviors, a mathematical property

applicable at least to hypothetical many-body interactions deserves mentioning. The basic issue concerns the existence of unit-Jacobian transformations within the many-body configuration space that leave the classical partition function unchanged, while fundamentally modifying kinetic properties. This involves invariance properties at all temperatures of the classical canonical configuration integral

$$Y\{\Phi\} = \int d\mathbf{R} \exp[-\Phi(\mathbf{R})/k_B T], \qquad 15.$$

subject to certain classes of interaction modifications. Suppose one has a continuous and differentiable transformation

$$\mathbf{R} \to \mathbf{R}'(\mathbf{R}), \qquad 16.$$

which distorts the configuration space by a simple stirring process, so that every initial hypervolume element $\delta\mathbf{R}$ becomes an equal-content (but possibly shape-distorted) final element $\delta\mathbf{R}'$ at a displaced location. Then the modified interaction function

$$\Phi'(\mathbf{R}) = \Phi[\mathbf{R}'(\mathbf{R})] \qquad 17.$$

yields exactly the same value for the canonical configuration integral at all temperatures:

$$Y\{\Phi'\} \equiv Y\{\Phi\}, \qquad 18.$$

because exactly the same contributions to the integral in Equation 15 are summed after the transformation as before. Hence, all thermodynamic properties (whether or not subject to the noncrystallization constraint) are identical for the two interactions. However, one must expect the Newtonian equations of motion, and thus kinetic properties, will not exhibit invariance. Such transformations preserve the numbers and potential energy values of all minima (inherent structures) as well as of saddle points of all orders.

An even more transparent class of potential energy transformations with the same Y invariance property has been proposed (85). It considers continuous and differentiable interactions $\Phi(\mathbf{R})$ that can be broken into modules in $\mathbf{R}$ space, specifically those that span unit cells of a regular $\mathbf{R}$ space lattice, where each of those modules has an assigned altitude, vanishing gradient at its edges, and fixed curvatures at those edges. The collection of modular units can be assembled in the $\mathbf{R}$ space in a wide variety of ways preserving overall continuity and differentiability, thus producing a great diversity of potential energy topographies. In particular, this diversity includes variation in the number of deep valleys or metabasins separated by kinetics-inhibiting barriers. However, the corresponding canonical configuration integrals Y are invariant to the way in which those given modular units are assembled to cover the $\mathbf{R}$ space. Once again the thermodynamic properties are decoupled from kinetic properties.

These in-principle examples of decoupling between thermodynamics and kinetics may have involved stepping well beyond the limits of realistic atomic or molecular interactions. However, it is currently unresolved whether this overstepping is generally inevitable. In those published theories of glass phenomena that claim strong coupling between thermodynamics and kinetics, no explicit criterion has yet been advanced as to precisely what classes of interaction functions should be allowed.

The spin-glass dynamical transitions at positive temperature exhibited by the Sherrington-Kirkpatrick, Potts, and p-spin models subject to Langevin kinetics are not accompanied by any thermodynamic distinguishing feature (Reference 9, section IV.B.1). This is not too surprising,

given that the spin interactions involved (infinite ranged, quenched random interactions) are quite unlike those for atomic or molecular glass formers. These dynamic transitions are associated with the spin systems falling into deep portions of their discrete potential energy landscapes, with barriers too high in the infinite system limit to allow kinetic escape, thus resulting in nonergodicity. Thus, upon cooling, different members of an ensemble for one of these spin-glass models would become trapped in different deep metabasins, and the distribution among those metabasins would amount to a nonvanishing configurational entropy at the dynamical transition temperature. Nevertheless, the analytical theory for these models shows that if a formal mechanism were present to create equilibration between these deep metabasins as temperature were reduced further, indeed a positive temperature would finally be attained at which entropy vanishes; i.e., they display ideal glass transitions.

A notable feature of the RFOT approach has been to identify what modifications would be necessary when transforming the model type from spin glass to conventional supercooled liquids of glass formers. The mosaic texture proposal that has emerged presumes that the length scale $\xi(T)$ measuring the mean size of local domains diverges at a positive temperature, and the resulting amorphous one-grain medium below that divergence is an ideal glass state. However, the current RFOT analysis does not offer a clear demonstration that the mechanically stable inherent structures that qualify for this presumed low-temperature state have subexponential enumeration with respect to system size N, which is the requirement that configurational entropy per particle vanish below the transition temperature in the large system limit.

Hard sphere and hard disk models have frequently been invoked for study of glass phenomena (e.g., 86, 87). For these models the interaction potential $\Phi(\mathbf{R})$ has only values 0 or $+\infty$, so temperature plays a rather minor role. Compression is the basic process to bypass equilibrium crystallization and place the system in an amorphous solid structure. If that compression is sufficiently extreme, and the system then is retained at fixed volume or area conditions, a many-sphere or many-disk system will become absolutely trapped configurationally by its particle nonoverlap requirements, resulting in vanishing self-diffusion constants and an inability to exhibit viscous flow. Although these limiting properties are reminiscent of ideal glass behavior, predictions for these hard-particle systems indicate that ideal glass behavior would actually be encountered at lower compressions, short of a strict geometric jamming state. One such prediction was based on molecular dynamics computer simulation results for binary hard disk systems by Speedy (88), where the disk diameter ratios were in the range 1.2 to 1.4. However, a subsequent binary disk simulation study for the 1.4 diameter ratio case found no evidence for an ideal glass transition (89).

The monodisperse hard sphere system has been analyzed theoretically by the replica method (90, 91). This approach has predicted an ideal glass transition in a density region below that of the random close packing density (coverage fraction ≈ 0.64, substantially below the close-packed crystal maximum ≈ 0.74). However, this replica method has invoked the hypernetted chain (HNC) approximation for amorphous states, and consequently is open to question. It deserves to be mentioned in passing that the coverage fraction of amorphous jammed sphere packings is demonstrably dependent on details of the compression protocol used to form them (92). Consequently, if ideal glass transitions were present, their quantitative details presumably should be protocol dependent. However, this feature thus far has not been explored.

The Kob-Andersen 80:20 Lennard-Jones binary mixture model (62, 93) has been the testing ground both for analytical and for simulational investigations of the existence of an ideal glass transition. Sciortino et al. (94) evaluated the density of states of inherent structure energies in a series of simulations, and extrapolated the entropy results to low temperature, thereby concluding that this model binary mixture would exhibit an ideal glass transition at a $T_K > 0$. Coluzzi

et al. (95, 96) applied a rather different method of analyzing and extrapolating computer simulation data for thermodynamic properties, but also concluded that the model produced a positive-temperature ideal glass transition.

The string-like excitation view of low-temperature glasses developed by Langer predicts a linear vanishing of configurational entropy at a positive temperature identified as a Kauzmann temperature (56, 57). Although this is not strictly the definition of an ideal glass transition involving the full entropy difference $\Delta S(T) \to 0$, as mentioned earlier, it seems reasonable to assume in this approximation that vibrational heat capacity contributions would lead to this latter criterion being obeyed at only a slightly shifted temperature. Several intuitively reasonable assumptions about the temperature-dependent statistics of the string-like excitations underlie this view of glasses, but more detailed analysis would be desirable to complete the case for or against a positive-temperature thermodynamic singularity.

6. LANDSCAPE CONSIDERATIONS

To provide some additional comments on thermodynamics and kinetics of glass formation, and specifically on the possibility of ideal glass transitions, it will be useful to review basic aspects of the $\Phi(\mathbf{R})$ multidimensional landscape topographies. The first explicit emphasis on the importance of those landscape features in controlling the dynamics of glass formers at low temperature appears to have been due to Goldstein (97). Subsequently, a mathematical formalism emerged, based on a steepest-descent mapping that connected any configuration point to a local or global minimum, i.e., an inherent structure configuration (98, 99). Thus the $\mathbf{R}$ configuration space for an N-particle system becomes uniquely divided (tiled) by steepest-descent basins, each one surrounding a single inherent structure configuration.

That the number of distinct (nonpermutation equivalent) inherent structures and their basins rises exponentially with system size N at constant density (28) leads to the possibility of representing the isochoric canonical partition function, and thus the Helmholtz free energy F, in terms of a simple quadrature over ϕ, the basin depth parameter on a per-particle basis. In the large system limit that is of interest in the present context, this has the following form ($\beta = 1/k_B T$):

$$-\beta F/N = \max_{\phi} \left[\sigma(\phi) - \beta\phi - \beta f_{\mathrm{v}}(\phi, \beta)\right]. \qquad 19.$$

Here, $\sigma(\phi)$ when appearing in the exponential format $\exp[N\sigma(\phi)]$ enumerates by depth inherent structures/basins that are permutation inequivalent, and $f_{\mathrm{v}}(\phi, \beta)$ is the mean intrabasin vibrational free energy per particle at a given temperature and basin depth. Both of these functions depend on particle density, left implicit for simplicity. The maximum indicated here simply identifies the set of basins dominantly occupied at the prevailing temperature and density. Equation 19 is applicable to the system's equilibrium thermodynamics when the enumeration covers the full configuration space. However, it is equally applicable to the metastable-system subspace of the configuration space after insertion of the crystal nucleation barrier as described earlier (Section 3; **Figure 2**), requiring then that enumeration function σ and vibrational free energy function f_{v} refer only to those inherent structures and basins in that subspace. Under this latter convention, vanishing of configurational entropy for a glass former amounts to the ϕ maximum identified in Equation 19 declining to the lower limit ϕ_{low} of the $\sigma(\phi)$ enumeration range at positive temperature, and that $\sigma(\phi_{low}) = 0$. As indicated earlier, this vanishing configurational entropy point would be very close to that at which $\Delta S = 0$. Although Equation 19 refers to isochoric (constant V) rather than isobaric (constant p) conditions, the existence or

nonexistence of an ideal glass transition under the latter circumstance can be inferred from the density-variation properties of the former condition.

The condition that locates the integrand maximum with respect to ϕ that is required in Equation 19 amounts to the following equality among derivatives:

$$d\sigma(\phi)/d\phi = \beta[1 + \partial f_v(\phi,\beta)/\partial\phi]. \qquad 20.$$

Numerical evidence has been accumulated indicating that vibrational free energy as expressed in the function $f_v(\phi,\beta)$ depends only in a weak nonsingular fashion on the basin depth parameter ϕ (91, 100). Consequently the right member of Equation 20 at low temperature will be dominated by β itself. Condition 20 requires matching of slopes for $\sigma(\phi)$ and $\beta[\phi + f_v(\phi,\beta)]$ when plotted versus ϕ, as indicated schematically in **Figure 4**.

An argument has been presented (101, 102) indicating that the depth distribution of inherent structures is at least approximately Gaussian for a specific binary mixture intended to represent nickel-phosphorus eutectic mixtures (103). If this simplification were valid, then the enumeration function $\sigma(\phi)$ would be an inverted parabola between its lower (ϕ_{low}) and upper (ϕ_{up}) limits of definition:

$$\sigma(\phi) = \sigma_0 - \sigma_1(\phi_\infty - \phi)^2 \quad (\phi_{low} \le \phi, \phi_\infty \le \phi_{up}); \qquad 21.$$

here σ_0 and σ_1 are density-dependent positive parameters, and the parabola maximum at $\phi = \phi_\infty$ is the location of the solution to Equation 21 in the infinite-temperature ($\beta = 0$) limit. [A random energy model constructed by Derrida also exhibits a parabolic enumeration function (104).] Because the slope of the parabolic function in Equation 21 remains positive at its lower limit ϕ_{low}, this would be a sticking point for Equation 19 at some positive temperature and all

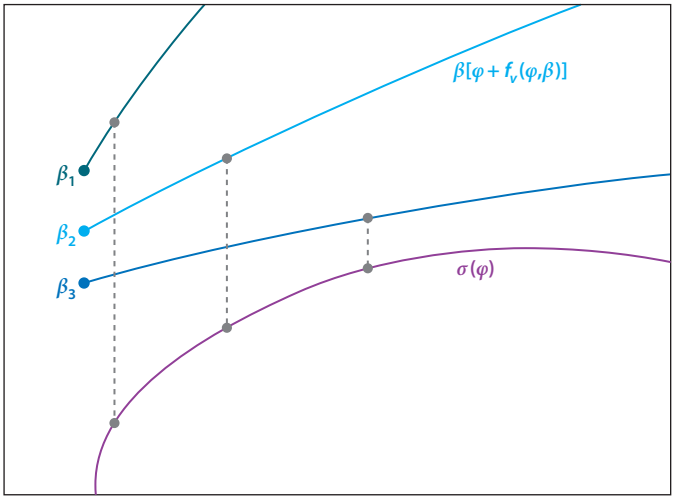

Figure 4

Slope matching conditions indicated by vertical lines at various temperatures $T = 1/k_B\beta$ for determination of the dominant basin depth ϕ. Here $\beta_1 > \beta_2 > \beta_3$, and $\sigma(\phi)$ is the temperature-independent enumeration function for inherent structures/basins as a function of their depth on a per-particle basis. A qualitatively similar view applies to the corresponding metabasin quantities after basin aggregation.

lower positive temperatures. That is, the configurational entropy would remain constant over this temperature interval. However it needs to be stressed that for this parabolic approximation, it is not sufficient to argue in favor of an ideal glass transition as thus far construed, because $\sigma(\phi_{low})$ might not vanish but be positive, and if so, configurational entropy would remain positive down to $T = 0$.

An alternative analysis has been proposed, pertaining presumably to all short-range interaction glass formers, that concludes $\sigma(\phi)$ must have a logarithmically diverging slope at the lower limit of the ϕ interval (105; 106, section IV):

$$\lim_{\phi \to \phi_{low}} d\sigma(\phi)/d\phi = +\infty. \qquad 22.$$

This qualitative but significant feature arises from enumeration of widely separated, thus essentially independent, local particle rearrangements in the lowest-potential energy amorphous inherent structures, each with an energy cost. Numerical simulation has provided some support for this approach (107). With respect to the slope matching criterion illustrated in **Figure 4**, Equation 22 if true would eliminate a positive-temperature singular point at which configurational entropy vanishes, and thus would eliminate the possibility of an ideal glass transition. This method of enumeration and energy assignment is analogous to, but a generalization of, that required for point defects such as vacancies and interstitials in an otherwise perfect crystal medium. For $\sigma(\phi)$ to retain a finite positive slope at ϕ_{low}, the analysis implies that the low-lying structural excitations would have to involve energy increments that increase without bound as the system size increases without bound.

An objection to conclusions produced by this last approach has been raised, based on the viewpoint that the states one should be concerned with are not the individual inherent structures and their basins, but rather contiguous combinations of basins forming metabasins (108). In particular, this would include in the same metabasin the low-energy two-level excitations that seem to be universally present in glasses near $T = 0$. In fact, a precisely defined extension of the topographic analysis leading to Equations 19 and 20 can easily be created in terms of a precise identification of metabasins, given a topographic coarse-graining energy ε. This process is carried out sequentially, starting with the deepest basin. First, identify all basins whose inherent structures can be connected to that lowest one by paths on the landscape, passing over shared saddle points, where those paths do not rise in potential energy anywhere along their length by more than the selected ε. Here, it will be assumed that ε is of molecular order and not proportional to system size. This connection process can include immediately neighboring basins sharing a boundary hypersurface with the lowest one, as well as noncontiguous basins, provided that the entire connecting path over one or more intervening basins does not anywhere exceed the height-change limit ε. The allowed set of connections then defines the metabasin, which includes that lowest basin serving as the starting point. Once that lowest metabasin has been constructed, the same algorithm is again applied to form a next-deepest metabasin, but using only the remainder set of basins not already aggregated. Repetition of this process eventually exhausts the original basin set, creating a tiling of the configuration space with ε-level metabasins. Although in principle it is arbitrary, ε could be chosen to exceed the majority of excitation energies for two-level degrees of freedom in the system of interest that would dominate its heat capacity at very low temperature.

Having identified ε-level metabasins, one can introduce an enumeration function $\overline{\sigma}(\phi)$for them, as well as a metabasin vibrational free energy function $\overline{f}_v(\phi, \beta)$, where once again the identifying variable ϕ refers to the depth on a per-particle basis of the bottom of the metabasin (i.e., the lowest included inherent structure energy). Because this metabasin construction process

does not eliminate any topographic information relevant to thermodynamics, the Helmholtz free energy can now equally well be written as the following extension of Equation 19:

$$-\beta F/N = \max_{\phi} \left[\overline{\sigma}(\phi) - \beta\phi - \beta \overline{f}_{\mathrm{v}}(\phi, \beta) \right]. \qquad 23.$$

Although the enumeration function $\overline{\sigma}$ declines as ε increases, that reduction is exactly compensated by a change in the vibrational free energy function $\overline{f}_{\mathrm{v}}$ to leave the free energy expression invariant. The maximum required in Equation 23 satisfies the corresponding extension of the earlier slope-matching condition, Equation 20, and **Figure 4** also serves to illustrate qualitatively satisfying that kind of condition.

Within the metabasin enumeration scheme, low-energy excitations now require at least ε. Again the crystal-phase point-defect analogy applies, and the same type of calculation as for $\varepsilon = 0$ concludes that $\overline{\sigma}$ has an infinite slope at the lower depth limit:

$$\lim_{\phi \to \phi_{low}} d\overline{\sigma}(\phi)/d\phi = +\infty. \qquad 24.$$

Consequently, the same conclusion emerges that configurational entropy (now computed on a metabasin occupancy standard) will not vanish at a positive temperature. But having stated that, this result does not eliminate the ideal glass transition as an empirically useful concept to organize measurements on deeply supercooled liquids, and in that respect it serves in a conceptual capacity analogous to that of spinodal curves for fluids carried into metastable states within vapor-liquid coexistence regions.

7. CONCLUSIONS

The development of theories of the glass transition is an active and often contentious area of contemporary condensed matter research. An abundance of divergent viewpoints exist that attempt to describe a well-defined set of physical phenomena. At present, such viewpoints fall into two broad categories. According to one, thermodynamics, in the form of an ideal glass transition, underlies and is responsible for the spectacular kinetic slowdown that characterizes deep supercooling and eventual vitrification. The alternative viewpoint is purely kinetic, and within it, conventional thermodynamics plays no role.

Precisely defined models, in particular the spin-glass models, have been shown to possess ideal glass transitions that occur at positive Kauzmann temperatures T_K. However, the interactions presented by these models differ fundamentally from those describing atomic and molecular glass formers that are electronic insulators. Although several approximate theories of the latter appear to describe qualitatively the mechanisms that underlie the powerful kinetic slowdown producing experimental glass transitions, they have not yet produced airtight arguments in favor of strict ideal glass transitions of the Kauzmann kind. Future research efforts must determine if unusual interactions mediated by mobile conduction electrons in metallic glasses, or by landscape complexity resulting from the high-molecular-weight limit for polymers, could provide exceptions.

But the deeper question remains one of causality. Even in the absence of a strict ideal glass transition, the fundamental issue remains whether the underlying cause of slowdown in structural relaxation is thermodynamic or kinetic. It would be a major theoretical accomplishment to identify logically airtight tests that could establish whether the glass transition in a given system or model is caused by a dearth of entropy or by purely kinetic constraints. This would enable a currently lacking unambiguous distinction between correlations, such as are observed between

kinetics and thermodynamics in many glass-forming systems, and causal relations. At present, we can only speculate whether the answer to this deep question turns out to be general or only system-specific.

DISCLOSURE STATEMENT

The authors are not aware of any affiliations, memberships, funding, or financial holdings that might be perceived as affecting the objectivity of this review.

ACKNOWLEDGMENTS

P.G.D. gratefully acknowledges the support of the National Science Foundation (grant CHE-1213343). Both authors thank Dr. Jeremy Palmer for figure preparation assistance.

LITERATURE CITED

1. Jäckle J. 1986. *Rep. Prog. Phys.* 49:171–231
2. Zarzycki J. 1991. *Glasses and the Vitreous State*. Cambridge: Cambridge Univ. Press
3. Ediger MD, Angell CA, Nagel SR. 1996. *J. Phys. Chem.* 100:13200–12
4. Angell CA, Ngai KL, McKenna GB, McMillan PF, Martin SW. 2000. *J. Appl. Phys.* 88:3113–57
5. Debenedetti PG, Stillinger FH. 2001. *Nature* 410:259–67
6. Binder K, Kob W. 2005. *Glassy Materials and Disordered Solids*. Singapore: World Sci.
7. Kivelson SA, Tarjus G. 2008. *Nat. Mater.* 7:831–33
8. Cavagna A. 2009. *Phys. Rep.* 476:51–124
9. Berthier L, Biroli G. 2011. *Rev. Mod. Phys.* 83:587–645
10. Kauzmann W. 1948. *Chem. Rev.* 43:219–56
11. Shumake NE, Garland CW. 1970. *J. Chem. Phys.* 53:392–407
12. Pauling L. 1935. *J. Am. Chem. Soc.* 57:2680–84
13. Angell CA. 1988. *J. Non-Cryst. Solids* 102:205–21
14. Angell CA. 1997. *J. Res. Natl. Inst. Stand. Technol.* 102:171–85
15. Lubchenko V, Wolynes PG. 2007. *Annu. Rev. Phys. Chem.* 58:235–66
16. Hecksher T, Nielson AI, Olsen NB, Dyre JC. 2008. *Nat. Phys.* 4:737–41
17. Adam G, Gibbs JH. 1965. *J. Chem. Phys.* 43:139–46
18. Berthier L. 2011. *Physics* 4:42
19. Gibbs JH, DiMarzio EA. 1958. *J. Chem. Phys.* 28:373–83
20. Kohlrausch R. 1854. *Ann. Phys. Chemie (Leipzig)* 91:179–214
21. Williams G, Watts DC. 1970. *Trans. Faraday Soc.* 66:80–85
22. Helfand E. 1983. *J. Chem. Phys.* 78:1931–34
23. Stillinger FH, Debenedetti PG. 2003. *Biophys. Chem.* 105:211–20
24. Greer AL. 2000. *Nature* 404:134–35
25. Anderson PW, Halperin BI, Varma CM. 1972. *Philos. Mag.* 25:1–9
26. Phillips WA. 1972. *J. Low Temp. Phys.* 7:351–60
27. Lubchenko V, Wolynes PG. 2003. *Proc. Natl. Acad. Sci. USA* 100:1515–18
28. Stillinger FH. 1999. *Phys. Rev. E* 59:48–51
29. Weber TA, Stillinger FH. 1985. *Phys. Rev. B* 32:5402–11
30. Vogel M, Doliwa B, Heuer A, Glotzer SC. 2004. *J. Chem. Phys.* 120:4404–14
31. Sastry S, Debenedetti PG, Stillinger FH. 1998. *Nature* 393:554–57
32. Bengtzelius U, Götze W, Sjölander A. 1984. *J. Phys. C Solid State Phys.* 17:5915–34
33. Leutheusser E. 1984. *Phys. Rev. A* 29:2765–73
34. Götze W. 1999. *J. Phys. Condens. Matter* 11:A1–45
35. Das SP. 2004. *Rev. Mod. Phys.* 76:785–851

36. Reichman DR, Charbonneau P. 2005. *J. Stat. Mech.: Theory Exp.* 2005: P05013
37. Mori H. 1965. *Prog. Theor. Phys.* 33:423–55
38. Zwanzig R. 2001. *Nonequilibrium Statistical Mechanics*. New York: Oxford Univ. Press
39. Singh Y, Stoessel JP, Wolynes PG. 1985. *Phys. Rev. Lett.* 54:1059–62
40. Eastwood MP, Wolynes PG. 2002. *Europhys. Lett.* 60:587–93
41. Kirkpatrick TR, Thirumalai D, Wolynes PG. 1989. *Phys. Rev. A* 40:1045–54
42. Sherrington D, Kirkpatrick S. 1978. *Phys. Rev. B* 17:4384–403
43. Gross DJ, Kanter I, Sompolinski H. 1985. *Phys. Rev. Lett.* 55:304–7
44. Gross DJ, Mezard M. 1984. *Nucl. Phys. B* 240:431–52
45. Xia XY, Wolynes PG. 2000. *Proc. Natl. Acad. Sci. USA* 97:2990–94
46. Stevenson JD, Wolynes PJ. 2005. *J. Phys. Chem. B* 109:15093–97
47. Bouchaud JP, Biroli G. 2004. *J. Chem. Phys.* 121:7347–54
48. Biroli G, Bouchaud J-P, Cavagna A, Grigera TS, Verrochio P. 2008. *Nat. Phys.* 4:771–75
49. Tarjus G, Kivelson SA, Nussinov Z, Viot P. 2005. *J. Phys. Condens. Matter* 17:R1143–82
50. Donati C, Glotzer SC, Poole PH, Kob W, Plimpton SJ. 1999. *Phys. Rev. E* 60:3107–19
51. Glotzer SC. 2000. *J. Non-Cryst. Solids* 274:342–55
52. Schrøder TB, Sastry S, Dyre JP, Glotzer SC. 2000. *J. Chem. Phys.* 112:9834–40
53. Gebremichael Y, Vogel M, Glotzer SC. 2004. *J. Chem. Phys.* 120:4415–27
54. Dzugutov M. 1992. *Phys. Rev. A* 46:R2984–87
55. Langer JS, Lemaitre A. 2005. *Phys. Rev. Lett.* 94:175701
56. Langer JS. 2006. *Phys. Rev. Lett.* 97:115704
57. Langer JS. 2006. *Phys. Rev. E* 73:041504
58. Garrahan JP, Chandler D. 2002. *Phys. Rev. Lett.* 89:035704
59. Merolle M, Garrahan JP, Chandler D. 2005. *Proc. Natl. Acad. Sci. USA* 102:10837–40
60. Chandler D, Garrahan JP. 2010. *Annu. Rev. Phys. Chem.* 61:191–217
61. Fredrickson GH, Andersen HC. 1984. *Phys. Rev. Lett.* 53:1244–47
62. Kob W, Andersen HC. 1993. *Phys. Rev. E* 48:4364–77
63. Jäckle J, Eisinger S. 1991. *Z. Phys. B Condens. Matter* 84:115–24
64. Garrahan JP, Chandler D. 2003. *Proc. Natl. Acad. Sci. USA* 100:9710–14
65. Biroli G, Bouchaud J-P, Tarjus G. 2005. *J. Chem. Phys.* 123:044510
66. Elmatad YS, Chandler D, Garrahan JP. 2010. *J. Phys. Chem. B* 114:17113–19
67. Ediger MD. 2000. *Annu. Rev. Phys. Chem.* 51:99–128
68. Weeks ER, Crocker JC, Levitt AC, Schofield A, Weitz DA. 2000. *Science* 287:627–31
69. Yamamoto R, Onuki A. 1998. *Phys. Rev. Lett.* 81:4915–18
70. Donati C, Glotzer SC, Poole PH. 1999. *Phys. Rev. Lett.* 82:5064–67
71. Parisi G. 1999. *J. Phys. Chem. B* 103:4128–31
72. Hodgdon JA, Stillinger FH. 1993. *Phys. Rev. E* 48:207–13
73. Stillinger FH, Hodgdon JA. 1994. *Phys. Rev. E* 50:2064–68
74. Stillinger FH, Hodgdon JA. 1996. *Phys. Rev. E* 53:2995–97
75. Berthier L, Biroli G, Bouchaud J-P, Cipeletti L, van Saarloos W. 2011. *Dynamical Heterogeneities in Glasses, Colloids, and Granular Media*. Oxford, UK: Oxford Univ. Press
76. Lačević N, Starr FW, Schrøder TB, Glotzer SC. 2003. *J. Chem. Phys.* 119:7372–87
77. Bennemann C, Donati C, Baschnagel J, Glotzer SC. 1999. *Nature* 399:246–49
78. Vogel M, Glotzer SC. 2004. *Phys. Rev. E* 70:061504
79. Widmer-Cooper A, Harrowell P, Fynewever H. 2004. *Phys. Rev. Lett.* 93:135701
80. Widmer-Cooper A, Perry H, Harrowell P, Reichman DR. 2008. *Nat. Phys.* 4:711–15
81. Malaspina D, Schulz EP, Frechero MA, Appignanesi GA. 2009. *Physica A* 388:3325–33
82. Ikeda A, Miyazaki K. 2011. *Phys. Rev. Lett.* 106:015701
83. Chang SS, Bestul AB. 1972. *J. Chem. Phys.* 56:503–16
84. Chang SS, Bestul AB. 1974. *J. Chem. Thermodyn.* 6:325–44
85. Stillinger FH, Debenedetti PG. 2002. *J. Chem. Phys.* 116:3353–61
86. Flenner E, Zhang M, Szamel G. 2011. *Phys. Rev. E* 83:051501

87. Charbonneau B, Charbonneau P, Tarjus G. 2012. *Phys. Rev. Lett.* 108:035701
88. Speedy RJ. 1999. *J. Chem. Phys.* 110:4559–65
89. Donev A, Stillinger FH, Torquato S. 2006. *Phys. Rev. Lett.* 96:225502
90. Mézard M, Parisi G. 1999. *Phys. Rev. Lett.* 82:747–50
91. Parisi G, Zamponi F. 2005. *J. Chem. Phys.* 123:144501
92. Jiao Y, Stillinger FH, Torquato S. 2011. *J. Appl. Phys.* 109:013508
93. Kob W, Andersen HC. 1995. *Phys. Rev. E* 51:4626–41
94. Sciortino F, Kob W, Tartaglia P. 1999. *Phys. Rev. Lett.* 83:3214–17
95. Coluzzi P, Parisi G, Verrocchio P. 2000. *Phys. Rev. Lett.* 84:306–9
96. Coluzzi B, Parisi G, Verrocchio P. 2000. *J. Chem. Phys.* 112:2933–44
97. Goldstein M. 1969. *J. Chem. Phys.* 51:3728–39
98. Stillinger FH, Weber TA. 1982. *Phys. Rev. A* 25:978–89
99. Stillinger FH, Weber TA. 1983. *Phys. Rev. A* 28:2408–16
100. Sciortino F, Kob W, Tartaglia P. 2000. *J. Phys. Condens. Matter* 12:6525–34
101. Büchner S, Heuer A. 1999. *Phys. Rev. E* 60:6507–18
102. Heuer A, Büchner S. 2000. *J. Phys. Condens. Matter* 12:6535–41
103. Weber TA, Stillinger FH. 1985. *Phys. Rev. B* 31:1954–63
104. Derrida B. 1981. *Phys. Rev. B* 24:2613–26
105. Stillinger FH. 1988. *J. Chem. Phys.* 88:7818–25
106. Debenedetti PG, Stillinger FH, Shell MS. 2003. *J. Phys. Chem. B* 107:14434–42
107. Sastry S. 2004. *J. Phys. Chem. B* 108:19698–702
108. Biroli G, Monasson R. 2000. *Europhys. Lett.* 50:155–61

Annual Review of Condensed Matter Physics

Volume 4, 2013

Contents

Errata

An online log of corrections to *Annual Review of Condensed Matter Physics* articles may be found at http://conmatphys.annualreviews.org/errata.shtml